Harla Journals

Harla Journal of Applied Science and Materials

Journal home page: https://journals.ddu.edu.et/index.php/HJASM

Harla journal of Applied Science and Materials

Synthesis and characterization of $BiVO_4$, $BiPO_4$, and $BiV_{0.5}P_{0.5}O_4$ nanomaterials prepared by solution combustion method

Nkomo Q[1], Yimamu A.U[2]*, Werta S.Z[2], Tshabalala K.G[1], and Motloung S.J[1]

[1]Department of Physics, University of the Free State (QwaQwa Campus), Private Bag X 13, Phuthaditjhaba, 9866, South Africa
[2]Department of Physics, Dire Dawa University, Dire Dawa, Ethiopia
**Corresponding author*

Abstract

Bismuth vanadate ($BiVO_4$), Bismuth phosphate ($BiPO_4$), and Bismuth vanadate phosphate ($BiV_{0.5}P_{0.5}O_4$) powder nanomaterials were successfully synthesized via the solution combustion method. Crystal structure, surface morphology, elemental composition, and stretching vibrations of the prepared powder nanoparticles were investigated by X-ray diffraction (XRD), scanning electron microscopy (SEM), energy dispersive X-ray spectroscopy (EDS), and Fourier transform infrared spectroscopy (FTIR). XRPD patterns confirmed the formation of the crystalline monoclinic phase. SEM images revealed agglomerated spherical-like nanoparticle morphology in all samples. The presence of the carbon (C), oxygen (O), bismuth (Bi), vanadium (V), and phosphorus (P) chemical elements was confirmed by EDS. $BiV_{0.5}P_{0.5}O_4$ was also verified by infrared stretching frequencies between 706 and 1068 cm^{-1}. The obtained results indicate that $BiV_{0.5}P_{0.5}O_4$ can be a potential material for photocatalysis applications.

Keywords/phrases: Bismuth vanadate; Bismuth phosphate; Nanomaterials; Photocatalysis; Solution combustion method

1. Introduction

Significant efforts have been made to find semiconductor materials with photocatalytic activity under visible light [1]. Metal oxides with high photocatalytic activity under visible-light illumination have been studied, such as $BaIn_2O_4$, $CaIn_2O_4$, $InVO_4$, TiO_2, $BiPO_4$, and $BiVO_4$ [1,2]. Oxide materials are suitable hosts for luminous dopant ions because of their favorable optical properties, including a high damage threshold and good non-linearity [3]. Oxide materials are widely used in various devices, including lamps, lasers, and phosphors for televisions [4,5]. Among various oxides studied, $BiVO_4$ and $BiPO_4$ have received special attention due to their intriguing features [1,6].

$BiVO_4$ is a promising photocatalyst for the destruction of organic pollutants in visible light with resistance to photo-corrosion and a narrow band gap (2.3-2.5 eV) [7,8]. Due to its strong thermal and chemical stability and the presence of components that are not hazardous to human health, $BiVO_4$ is an environmentally friendly photocatalyst [9,7].

**Corresponding author: A.U Yimamu; email: ahed.dilla@gmail.com ; Cell phone: +251930509797*

Received: July 2024; Received in revised form: November 2024; Accepted: December 2024

Monoclinic $BiVO_4$, achieves higher photocatalytic performance, high stability, and low cost than the other two crystal phases [9,11]. However, due to the inability of monoclinic $BiVO_4$ to effectively separate photogenerated electron-hole pairs, its actual photocatalytic activity is not ideal [12].

However, $BiPO_4$ has received much attention due to its cost-effectiveness, highly stable chemical structure, non-toxicity, and excellent optical, electronic, and photocatalytic properties [13-15]. As a wide band-gap material, $BiPO_4$ has a weak response to visible light and low energy utilization, resulting in low catalytic activity of visible light, severely limiting its wider application [13]. Several strategies have already been developed to overcome such shortcomings, such as non-transition metal ion doping and narrower band gap semiconductor couplings [13-14].

The two hosts $BiVO_4$ and $BiPO_4$ rarely mix to form vanadate-phosphate multicomponent structures. This is achieved by partially replacing $[VO_4]^{3-}$ with $[PO_4]^{3-}$ ions or $[PO_4]^{3-}$ with $[VO_4]^{3-}$ to form so-called multicomponent systems. Bismuth vanadate phosphate crystallizes in a monoclinic structure depending on the vanadium-to-phosphorus molar ratio, the oxidation state, and the fabrication temperature [16,17]. $BiVO_4$ and $BiPO_4$ material have been previously prepared using various synthetic methods such as sol-gel, co-precipitation, combustion, hydrothermal, facile microwave, and solid-state [19-23]. Among them, the solution combustion method was used to synthesize $BaVO_4$, $BiPO_4$, and $BiV_{0.5}P_{0.5}O_4$ nanopowders. The solution combustion method was chosen because of its advantages, such as versatility, easy incorporation of dopant ions, fast and self-sustaining reaction, and lower energy consumption [7,19,25].

2. Experimental

2.1. Synthesis

The synthesis of $BiV_{0.5}P_{0.5}O_4$ nanomaterial was carried out using urea as fuel in a solution combustion method. As part of normal preparation, stoichiometric amounts of ammonium metavanadate (NH_4VO_3), ammonium dihydrogen phosphate ($NH_4H_2PO_4$), bismuth (III) nitrate pentahydrate (Bi $(NO_3)_3.5H_2O$) and urea (CH_4N_2O) were dissolved in deionized water. After vigorous stirring, a homogeneous solution was obtained. The homogeneous mixture was transferred to a crucible. The solution in a crucible was then placed in a furnace preheated to 600 ± 10 °C for 15 minutes. As a result of this high temperature, the water evaporated, and the reagents decomposed and released gases. The crucible was left in the furnace for 24 hours until it cooled down before it was taken out of the furnace and placed at room temperature. The resulting combustion ashes were ground gently using a pestle and mortar. This method was used for the preparation of $BiVO_4$ and $BiPO_4$ powder samples; the synthesized nanopowders were ready for characterization.

2.2. Characterizations

XRD analysis of the prepared powder nanomaterial was performed to determine the phase structure, purity, and crystallinity. The XRD used was Cu K_α radiation (λ =0.15418 nm, 40 kV, and 40 mA). The surface morphology and chemical composition of the samples were examined using the TESCAN VESA 3 SEM Oxford X-MAX EDS. A Nicolet 6700 Fourier Transform

infrared (FTIR) spectrometer was used to analyze the vibration stretching modes frequencies of the samples.

3. Results and Discussions

3.1. X-ray diffraction

XRPD analysis was performed on powder nanomaterials to determine the phase structure, purity, and crystallinity [24]. Figure 1A shows XRPD diffractograms of $BiVO_4$, $BiPO_4$, and $BiV_{0.5}P_{0.5}O_4$ nanoparticles. XRPD results revealed that diffraction peaks of the $BiVO_4$ sample are well indexed with the monoclinic crystalline structure according to the Joint Committee on Powder Diffraction Standards (JCPDS)-14-0688. $BiV_{0.5}P_{0.5}O_4$ diffraction peaks correspond with XRPD peaks observed in $BiVO_4$ and $BiPO_4$ samples. It is worth noting that the XRPD peaks indicate the formation of the monoclinic $BiV_{0.5}P_{0.5}O_4$ crystal structure. $BiV_{0.5}P_{0.5}O_4$ diffractograms are well indexed with the structure of JCPDS-14-0688 with a slight shift towards the low angles compared to the structure of JCPDS-15-0767 in Figure 1 A. This shift may be due to stress because of the difference in the ionic radius of vanadium ($\sim 0.54A°$) and phosphorus ($\sim 0.35A°$) [24]. The peaks are sharp and slightly broadened, indicating a well-crystalline powder with a small crystallite size [26]. There is good agreement between the peaks of $BiPO_4$ obtained from XRPD and the monoclinic structure of JCPDS-15-0767.

The plot of $4sin\,\theta$ vs $\beta cos\,\theta$ of $BiV_{0.5}P_{0.5}O_4$ sample is shown in Figure 1B. According to the Williamson-Hall equation, the crystallite size of $BiV_{0.5}P_{0.5}O_4$ was estimated to be 20.23 nm while the micro-strain was estimated to be 0.0118 nm using the Stokes-Wilson formula in equation 2. The Williamson-Hall (equation 1) is given by:

$$\beta cos\,\theta = 4\varepsilon sin\,\theta + \frac{k\lambda}{D} \qquad (1)$$

$$\varepsilon = \frac{\beta}{4Tan\,\theta} \qquad (2)$$

Where D is the crystallite size, ε is the lattice strain, λ is the wavelength, β is the full width at half maximum intensity, and θ is the diffraction angle at the peak position. The lattice parameters were calculated using Miller indices (002), (200), (-121), (012), and (020).

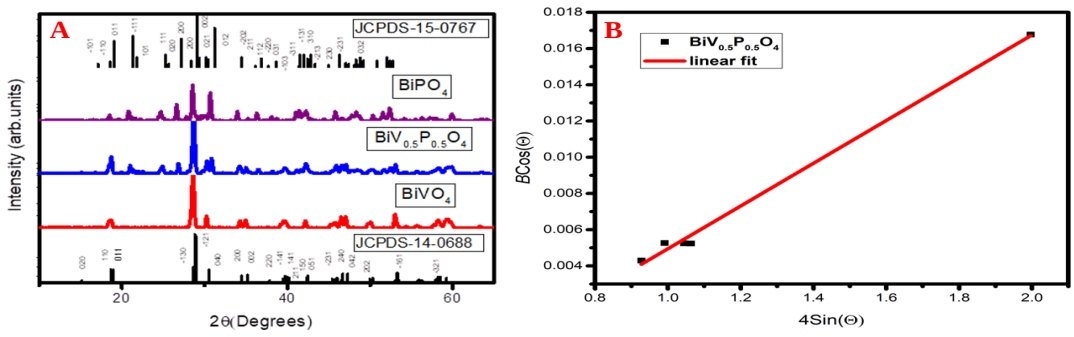

Figure 1: (a) XRPD diffractograms of pure $BiVO_4$, $BiPO_4$, and $BiV_{0.5}P_{0.5}O_4$ nanomaterials, (b) the Williamson-Hall plot of $BiV_{0.5}P_{0.5}O_4$ powder samples.

Table 1**:** Structural lattice parameters of the prepared powders nanomaterials.

Lattice parameter (Å)	a	b	c
$BiVO_4$	5.20	11.70	5.09
$BiV_{0.5}P_{0.5}O_4$	6.84	5.11	6.40
$BiPO_4$	6.75	6.93	6.47

3.2 Scanning electron microscopy (SEM)

SEM was used to examine the nanostructures and study the surface morphology of the samples [27].

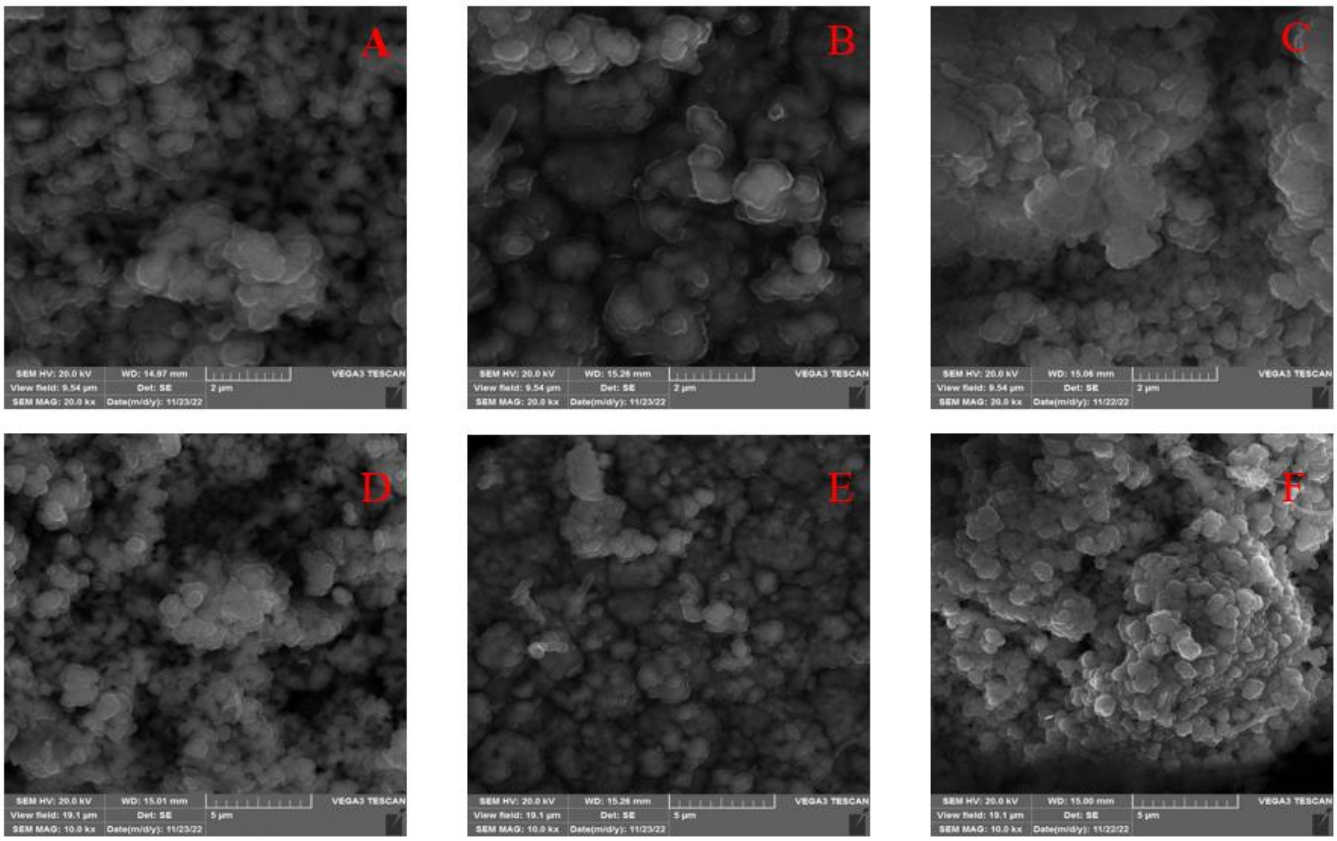

Figure 3: SEM images of as-prepared $BiVO_4$, $BiPO_4$, and $BiV_{0.5}P_{0.5}O_4$ powder nanomaterial.

Figure 3 shows the spherical surface morphology of $BiVO_4$, $BiPO_4$, and $BiV_{0.5}P_{0.5}O_4$ powders. Agglomeration of spherical-shaped particles is visible from the SEM images in Figure 3. This agglomeration may be caused by the overlapping of small and middle particles caused by weak surface forces (soft agglomerates) or strong chemical bonds (hard agglomerates). The surface contains voids that could have resulted from the evolution of gaseous species during combustion [28]. As the solution combustion process proceeds, endothermic reactions result in the decomposition and removal of carbon dioxide (CO_2) and water (H_2O), which varies significantly depending on the precursor ingredients and the ratio of Bismuth to urea ratio [27]. Therefore, voids are attributed to these gases that evolved during combustion [27]. In Figure 3, A, B, and C,

show higher magnification images with primary spherical-shaped particles, while D, E, and F, are with lower magnification with secondary particles.

3.3 Energy-dispersive X-ray spectroscopy (EDS)

Figure 4A depicts the EDS spectrum of $BiV_{0.5}P_{0.5}O_4$ powder nanoparticles. The EDS spectrum indicates the presence of Carbon(c), oxygen (O), bismuth (Bi), Vanadium (V), and Phosphorus(P) elements in the sample [29]. EDS detected the percentage of the C element which is due to the carbon coating used to mount the sample. The EDS elemental mapping of $BiV_{0.5}P_{0.5}O_4$ powder nanomaterial shows the uniform distribution of the elements on the surface. This uneven distribution might be due to the area of interest during EDS elemental mapping measurement. However, the elements detected in EDS are elements observed in XRPD indicating the formation of $BiV_{0.5}P_{0.5}O_4$ nanoparticles.

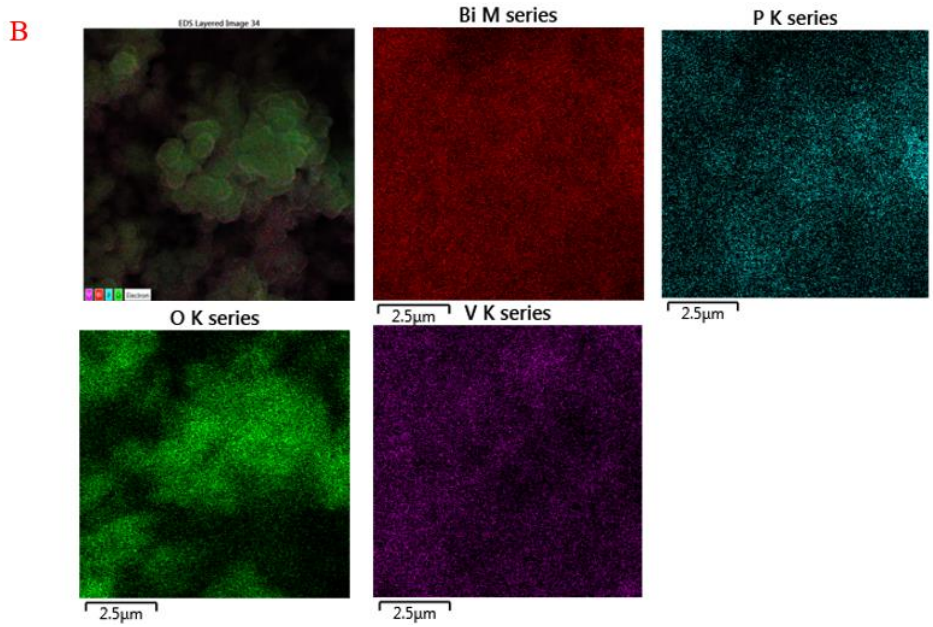

Figure 4: (a) EDS spectrum, and (b) EDS elemental mapping of $BiV_{0.5}P_{0.5}O_4$ powder nanoparticles.

3.4 Fourier-transform infrared spectroscopy (FTIR)

The FTIR technique was used to analyze $BiVO_4$, $BiPO_4$, and $BiV_{0.5}P_{0.5}O_4$, which provides information on all the functional groups of amorphous and crystalline mixtures of the compound, as each group generates a unique molecular vibrational spectrum [7]. Figure 5 shows FTIR transmittance spectra recorded at room temperature in a range of 625- 4000 cm^{-1}. Figure 5A shows the FTIR spectrum of $BiVO_4$ with both asymmetric and symmetric stretching vibrations of V-O bonds of VO_4^{3-} at 700- 900 cm^{-1} [7]. The presence of absorption peak at 1046- 3280 cm^{-1} in pure $BiVO_4$ samples is attributed to H_2O molecules and hydroxyl ions adsorbed on the photocatalyst surface [30]. Figure 5B shows FTIR spectra of $BiPO_4$ with strong absorption peaks between 907 and 1068 cm^{-1} which are attributed to P-O bond stretches of PO_4^{3-} [31]. The combination of $BiVO_4$ and $BiPO_4$ results in a multicomponent $BiV_{0.5}P_{0.5}O_4$ structure, different absorption peaks are observed at 706, 819, 990, and 1068 cm^{-1}, corresponding to the V-O bond

stretches of VO_4^{3-} and P-O bonds of PO_4^{3-} in Figure 5C. This analysis indicates the formation of $BiV_{0.5}P_{0.5}O_4$ as a new material.

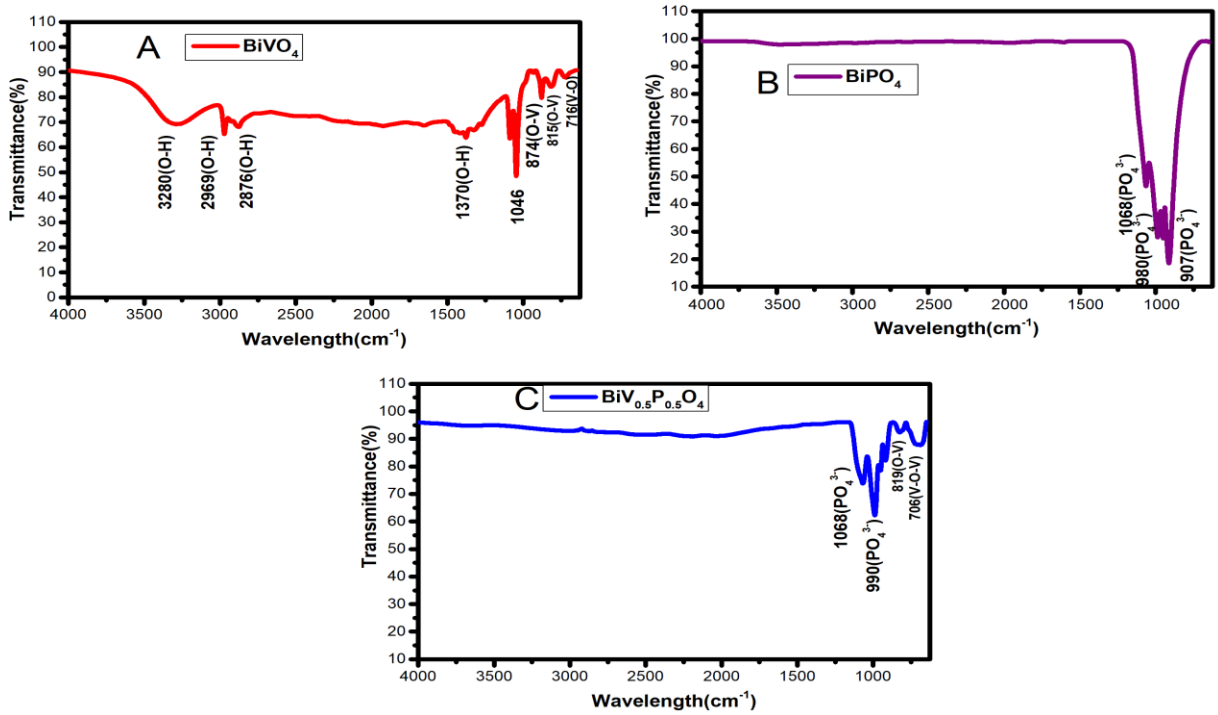

Figure 5: FTIR spectrum of (a) $BiVO_4$, $BiPO_4$, and (c) $BiV_{0.5}P_{0.5}O_4$ powder samples.

4. Conclusion

The solution combustion method was successfully used to prepare $BiVO_4$, $BiPO_4$, and $BiV_{0.5}P_{0.5}O_4$ powder nanoparticles. XRPD result showed the formation of the monoclinic phase of $BiVO_4$ and $BiPO_4$. On the other hand, the XRPD peaks of $BiV_{0.5}P_{0.5}O_4$ agree well with those of $BiVO_4$ and $BiPO_4$, indicating that the phosphate ions were successfully incorporated into $BiVO_4$. SEM micrographs showed that granules were formed from an agglomeration of spherical-shaped particles. EDS results confirmed the presence of major elements in the sample. FTIR was used to observe stretching vibrational modes. This analysis indicates the formation of $BiV_{0.5}P_{0.5}O_4$ as a new material that can be alternatively used in photocatalysis applications.

Acknowledgments

The author would like to acknowledge the support of the Physics Department at the University of the Free State (QwaQwa campus).

References

[1] U. M. García Pérez, S. Sepúlveda-Guzmán, A. Martínez-De La Cruz and U. Ortiz Méndez, "Photocatalytic activity of BiVO4 nanospheres obtained by solution combustion synthesis using sodium carboxymethylcellulose," *J Mol Catal A Chem*, vol. 335, no. 1–2, pp. 169–175, Feb. 2011, doi: 10.1016/J.MOLCATA.2010.11.030.

[2] S. Perween *et al.*, "Improving the Photocatalytic activity for Hydrogen Evolution of LaBaInO4 via Topochemical Fluorination to LaBaInO3F2," May 2022, doi: 10.26434/CHEMRXIV-2022-0DNSZ.

[3] P. v. Raleaooa, A. Roodt, G. G. Mhlongo, D. E. Motaung, and O. M. Ntwaeaborwa, "Analysis of the structure, particle morphology and photoluminescent properties of ZnS:Mn2+ nanoparticulate phosphors," *Optik - International Journal for Light and Electron Optics*, vol. 153, pp. 31–42, Jan. 2018, doi: 10.1016/J.IJLEO.2017.09.120.

[4] C. Zhang, H. Chu, Z. Pan, H. Pan, S. Zhao, and D. Li, "Nonlinear optical properties of porous monoclinic BiVO4 at 2.3 μm for the passively Q-switching laser," *Opt Laser Technol*, vol. 157, p. 108753, Jan. 2023, doi: 10.1016/J.OPTLASTEC.2022.108753.

[5] V. Dimitrov and T. Komatsu, "Electronic polarizability, optical basicity and non-linear optical properties of oxide glasses," *J Non Cryst Solids*, vol. 249, no. 2–3, pp. 160–179, Jul. 1999, doi: 10.1016/S0022-3093(99)00317-8.

[6] R. Kumar *et al.*, "Recent progress in emerging BiPO4-based photocatalysts: Synthesis, properties, modification strategies, and photocatalytic applications," *J Mater Sci Technol*, vol. 108, pp. 208–225, May 2022, doi: 10.1016/J.JMST.2021.08.053.

[7] A. Phuruangrat, S. Wannapop, T. Sakhon, B. Kuntalue, T. Thongtem, and S. Thongtem, "Characterization and photocatalytic properties of BiVO4 synthesized by combustion method," *J Mol Struct*, vol. 1274, p. 134420, Feb. 2023, doi: 10.1016/J.MOLSTRUC.2022.134420.

[8] H. Gemechu *et al.*, "Semiconductor-Based Photocatalytic Oxygen Evolution Performance for Water Splitting: Light-Driven Energy Conversion and Storage," *Green Energy and Technology*, pp. 263–320, 2023, doi: 10.1007/978-981-19-6748-1_5/COVER.

[9] K. Lv, D. Wan, D. Zheng, Y. Qin, and Y. Lv, "Enhancement of visible light photocatalytic activity of BiVO4 by polypyrrole modification," *J Alloys Compd*, vol. 872, p. 159597, Aug. 2021, doi: 10.1016/J.JALLCOM.2021.159597.

[10] T. Senasu, S. Youngme, K. Hemavibool, and S. Nanan, "Sunlight-driven photodegradation of oxytetracycline antibiotic by BiVO4 photocatalyst," *J Solid State Chem*, vol. 297, p. 122088, May 2021, doi: 10.1016/J.JSSC.2021.122088.

[11] K. Lenczewska, D. Szymański, and D. Hreniak, "Control of optical properties of luminescent BiVO4:Tm3+ by adjusting the synthesis parameters of microwave-assisted hydrothermal method," *Mater Res Bull*, vol. 154, p. 111940, Oct. 2022, doi: 10.1016/J.MATERRESBULL.2022.111940.

[12] G. Zhao, W. Liu, J. Li, Q. Lv, W. Li, and L. Liang, "Facile synthesis of hierarchically structured BiVO4 oriented along (010) facets with different morphologies and their photocatalytic properties," *Appl Surf Sci*, vol. 390, pp. 531–539, Dec. 2016, doi: 10.1016/J.APSUSC.2016.08.126.

[13] Y. Naciri *et al.*, "Recent progress on the enhancement of photocatalytic properties of BiPO4 using π–conjugated materials," *Adv Colloid Interface Sci*, vol. 280, p. 102160, Jun. 2020, doi: 10.1016/J.CIS.2020.102160.

[14] Y. Naciri *et al.*, "Recent progress on the enhancement of photocatalytic properties of BiPO4 using π–conjugated materials," 2020. doi: 10.1016/j.cis.2020.102160.

[15] R. Li, W. Yuan, Y. Hu, and Y. Zeng, "Photoelectrochemical aptasensor for sensitively detecting S-Propranolol based on Au NPs modified g-C3N4/BiPO4 heterojunction," *Sens Actuators A Phys*, vol. 363, 2023, doi: 10.1016/j.sna.2023.114737.

[16] W. J. Yu, Y. Cheng, T. Zou, Y. Liu, K. Wu, and N. Peng, "Preparation of BiPO4-Polyaniline Hybrid and its Enhanced Photocatalytic Performance," *https://doi.org/10.1142/S1793292018500091*, vol. 13, no. 1, Feb. 2018, doi: 10.1142/S1793292018500091.

[17] A. Gupta *et al.*, "Up-conversion hybrid nanomaterials for light- and heat-driven applications," *Prog Mater Sci*, vol. 121, p. 100838, Aug. 2021, doi: 10.1016/J.PMATSCI.2021.100838.

[18] P. Patra and K. Annapurna, "Transparent tellurite glass-ceramics for photonics applications: A comprehensive review on crystalline phases and crystallization mechanisms," *Prog Mater Sci*, vol. 125, p. 100890, Apr. 2022, doi: 10.1016/J.PMATSCI.2021.100890.

[19] A. Mayavan, A. Kannan, and S. Gandhi, "Photoluminescence assessment of Ba2-xEuxSiO4 phosphor prepared through a solid phase reaction technique using silica nanoparticles as a precursor," *Mater Chem Phys*, vol. 288, p. 126329, Sep. 2022, doi: 10.1016/J.MATCHEMPHYS.2022.126329.

[20] A. Joshi, P. Chand, and V. Singh, "Electrochemical and optical study of BiPO4nanostructures for energy storage applications," in *Materials Today: Proceedings*, 2020. doi: 10.1016/j.matpr.2020.02.153.

[21] A. Phuruangrat, S. Wannapop, T. Sakhon, B. Kuntalue, T. Thongtem, and S. Thongtem, "Characterization and photocatalytic properties of BiVO4 synthesized by combustion method," *J Mol Struct*, vol. 1274, 2023, doi: 10.1016/j.molstruc.2022.134420.

[22] J. P. Deebasree, V. Maheskumar, and B. Vidhya, "Investigation of the visible light photocatalytic activity of BiVO4 prepared by sol gel method assisted by ultrasonication," *Ultrason Sonochem*, vol. 45, 2018, doi: 10.1016/j.ultsonch.2018.02.002.

[23] O. M. Pardeshi, A. B. Gite, G. H. Jain, B. M. Palve, and A. V. Patil, "Sol gel auto-combustion synthesis of bismuth vanadate (BiVO4) nanoparticles and its supercapacitor applications," *Journal of Materials Science: Materials in Electronics*, vol. 34, no. 26, 2023, doi: 10.1007/s10854-023-11229-5.

[24] S. J. Motloung, M. A. Lephoto, K. G. Tshabalala, and O. M. Ntwaeaborwa, "Combustion synthesis and characterization of MV0.5P0.5O4: Sm3+, Tm3+ (M = Gd, La, Y)," *Physica B Condens Matter*, vol. 535, pp. 211–215, Apr. 2018, doi: 10.1016/J.PHYSB.2017.07.038.

[25] Y. R. Parauha, V. Sahu, and S. J. Dhoble, "Prospective of combustion method for preparation of nanomaterials: A challenge," 2021. doi: 10.1016/j.mseb.2021.115054.

[26] T. Carbonati, C. Cionti, E. Cosaert, B. Nimmegeers, D. Meroni, and D. Poelman, "NIR emitting GdVO4:Nd nanoparticles for bioimaging: The role of the synthetic pathway," *J Alloys Compd*, vol. 862, p. 158413, May 2021, doi: 10.1016/J.JALLCOM.2020.158413.

[27] M. A. Lephoto, K. G. Tshabalala, S. J. Motloung, G. H. Mhlongo, and O. M. Ntwaeaborwa, "Photoluminescence studies of green emitting BaB8O13: Bi3+ phosphors prepared by solution combustion method," *J Lumin*, vol. 200, pp. 94–102, Aug. 2018, doi: 10.1016/J.JLUMIN.2018.04.014.

[28] A. Malathi, P. Arunachalam, V. S. Kirankumar, J. Madhavan, and A. M. Al-Mayouf, "An efficient visible light driven bismuth ferrite incorporated bismuth oxyiodide (BiFeO3/BiOI) composite photocatalytic material for degradation of pollutants," *Opt Mater (Amst)*, vol. 84, pp. 227–235, Oct. 2018, doi: 10.1016/J.OPTMAT.2018.06.067.

[29] M. He, N. Jia, X. Liu, Y. Shen, and L. Zuo, "Abnormal chemical composition fluctuations in multi-principal-element alloys induced by simple cyclic deformation," *J Mater Sci Technol*, vol. 113, pp. 287–295, Jun. 2022, doi: 10.1016/J.JMST.2021.08.075.

[30] M. Noor, F. Sharmin, M. A. A. Mamun, S. Hasan, M. A. Hakim, and M. A. Basith, "Effect of Gd and Y co-doping in BiVO4 photocatalyst for enhanced degradation of methylene blue dye," *J Alloys Compd*, vol. 895, p. 162639, Feb. 2022, doi: 10.1016/J.JALLCOM.2021.162639.

[31] F. Yang *et al.*, "The effects of pH on reactive species formation in moxifloxacin photocatalytic degradation via BiPO4 prismatic," *Opt Mater (Amst)*, vol. 133, p. 112892, Nov. 2022, doi: 10.1016/J.OPTMAT.2022.112892.